Laboratory study of the heterogeneous ice nucleation on black carbon containing aerosol

Leonid Nichman[1, 4], Martin Wolf[2], Paul Davidovits[1], Timothy B. Onasch[1, 4], Yue Zhang[1, 4, 5], Doug R. Worsnop[4], Janarjan Bhandari[6], Claudio Mazzoleni[6], Daniel J. Cziczo[2, 3]

[1]Department of Chemistry, Boston College, Chestnut Hill, MA, 02467, USA
[2]Department of Earth, Atmospheric and Planetary Sciences, Massachusetts Institute of Technology, Cambridge, MA, USA
[3]Department of Civil and Environmental Engineering, Massachusetts Institute of Technology, Cambridge, MA, USA
[4]Aerodyne Research, Inc, Billerica, MA, 01821, USA
[5]Department of Environmental Science and Engineering, Gillings School of Global Public Health, University of North Carolina at Chapel Hill, Chapel Hill, NC, 27599, USA
[6]Department of Physics and Atmospheric Sciences Program, Michigan Technological University, Houghton, MI, 49931, USA

Correspondence to: Leonid Nichman (nichman@bc.edu)

Abstract. Black carbon (BC) particles are generated in the incomplete combustion of fossil fuels, biomass, and biofuels. These airborne particles affect air quality, human health, and climate. At present, the climate effects of BC particles are not well understood. Their role in cloud formation is obscured by their chemical and physical variability, and by the internal mixing states of these particles with other compounds. The current study focuses on laboratory measurements of the effectiveness of BC-containing aerosol in the formation of ice crystals in cirrus clouds. Ice nucleation in field studies is often difficult to interpret. Nonetheless, most field studies seem to suggest that BC particles are not efficient ice nuclei (IN). On the other hand, laboratory measurements show that in some cases, BC particles can be highly active IN. By working with well-characterized BC-containing particles, our aim is to systematically establish the factors that govern the IN activity of BC.

We examine ice nucleation on BC-containing particles under cirrus cloud conditions, commonly understood to be deposition mode ice nucleation. We study a series of well-characterized commercial carbon black particles with varying morphologies and surface chemistries, as well as ethylene flame-generated combustion soot. The carbon black particles used in this study are proxies for atmospherically relevant BC aerosols. These samples were characterized by electron microscopy, mass spectrometry, and optical scattering measurements. Ice nucleation activity was systematically examined in the temperature range from 217 – 235 K, using a SPectrometer for Ice Nuclei (SPIN) instrument, which is a continuous flow diffusion chamber coupled with instrumentation to measure light scattering and polarization. To study the effect of coatings on IN, the BC-containing particles were coated with organic acids found in the atmosphere, namely, stearic acid, cis-pinonic acid, and oxalic acid.

The results show significant variations in ice nucleation activity as a function of size, morphology and surface chemistry of the BC-containing particles. The measured IN activity dependence on temperature and the physicochemical properties of the BC-containing particles are consistent with an ice nucleation mechanism of pore condensation followed by freezing. Coatings and surface oxidation modify the initial ice nucleation ability of BC-containing aerosol. Depending on the BC material and the coating, both inhibition and enhancement in IN activity

were observed. Our measurements at low temperatures complement published data, and highlight the capability of some BC particles to nucleate ice under low supersaturation conditions. These results are expected to help refine theories relating to soot IN activation in the atmosphere.

1 Introduction

5   Ice nucleating particle (INP) types in the atmosphere vary widely across the globe. Although their number concentrations are typically low, their atmospheric impact, governing ice cloud formation and properties, is significant. The role of soot in atmospheric ice nucleation (IN) processes remains poorly understood. The indirect effect of soot particles, particularly on upper tropospheric cirrus clouds and aviation contrails, may result in either positive or negative forcing depending on the type of soot and the ambient conditions (Zhou & Penner, 2014). While

10   field studies tend to find limited evidence for soot particles acting as efficient INP, laboratory studies have shown that some soot particles can initiate ice nucleation. The increasing number concentration of emitted soot particles since the preindustrial times (Bond et al., 2013; Lavanchy et al., 1999), the emissions of soot particles in the upper troposphere from aviation (Lee et al., 2009), and estimates that the concentration of soot will remain high in the near future (Gasser et al., 2017) underscore the importance in understanding the efficiency of soot particles acting as ice

15   nucleating particles.

Current field results are inconclusive about the efficiency of soot particles in initiating ice nucleation. Recently, Chen et al. (2018) collected aerosol samples in a highly polluted environment and subsequently measured their IN activity. The soot samples showed no correlation between IN activity and BC fraction of the aerosol. Similarly, low activity was found by Pratt et al. (2009), and Eriksen-Hammer et al. (2018). Other field studies showed higher IN activity of

20   soot (Petzold et al., 1998). Phillips et al. (2013) suggested that black carbon is a major type of INP in clouds, however they couldn't rule out that another INP species, internally mixed with soot, might have nucleated the observed ice. Likewise, Levin et al. (2014) concluded that fires could be a significant source of INP in clouds. While in these studies the amount of soot INP appears to be low, it does not imply low IN activity for soot. For example, Ladino et al. (2017) reported that measured concentration of ice crystals in tropical mesoscale convective systems exceeded the

25   concentration of INP by several orders of magnitude. This observation suggests that ice multiplication originates from fragmentation of primary ice crystals, is a plausible explanation for the observed concentration gap between INP and ice crystals.

Laboratory studies of ice nucleation by soot particles in the cirrus cloud regime reveal a widespread IN activity (e.g. Kulkarni et al. (2016); Friedman et al. (2011); China et al. (2015a); Ullrich et al. (2017); Cziczo et al. (2016); Demott

30   et al. (2009); Kanji et al. (2017); Hoose and Möhler, (2012)). Laboratory studies by DeMott et al. (1999) and Kärcher & Lohmann (2003) have shown that the ice can form on soot, similarly to the formation of visible contrails (condensation trails) behind aircraft. The so-called soot-induced cirrus cloud formation is also described by Jensen and Toon (1997) and Kärcher et al. (2007), where the exhaust soot disperses to form or modify cirrus cloud. Persistent linear contrails and induced-cirrus cloudiness, also known as aviation-induced cloudiness, are predicted to increase in

35   the coming years as the importance of aviation, and its consequent climate impact, will continue to increase (Lee et al., 2009). Other laboratory experiments indicate that the heterogeneous IN activity of soot in the deposition mode

Atmospheric
Chemistry
and Physics
Discussions

may be minimal (e.g. DeMott 1990, Kärcher et al., 2007, Kanji and Abbatt, 2006) and therefore would not contribute to cirrus coverage.

Both field and laboratory studies indicate that coating of soot particles in the atmosphere, in most cases, decreases their IN activity compared to their bare counterparts (Kärcher et al., 2007). Further, numerous soot types have shown

5   high IN activity in the deposition mode if they have a sufficiently low organic carbon content and are uncoated (Crawford et al., 2011).

Modeling INPs requires quantitative relationships that governs the IN activity. Two approaches to explain the IN data are commonly used: a stochastic description based on classical nucleation theory and a deterministic or singular description (Knopf et al, 2018). For the latter, the pragmatic description of active site density (n_s), is often used (Vali,

10   2014). Active site density is the fraction of the ice particles out of the total aerosol concentration divided by the averaged particle surface area. This approach describes the density of active sites (n_s) as a function of temperature, allowing for comparison between measurements and for modeling purposes, but does not take into account the kinetics (i.e. time dependence) of nucleation (e.g. Marcolli, 2014; Wagner et al 2016; Ullrich et al 2017; Kanji et al 2017; Kiselev et al. 2017; Campbell 2017). In this study, we report results suitable for both types of parameterizations, time

15   dependent (Sect. 3.1) and time independent (Sect. 3.2), for INP representation in models.

A kinetic-based mechanism referred to as pore condensation and freezing (PCF) provides, at least in part, a possible explanation for the widespread IN activity observed for soot particles. This mechanism was formulated to explain ice nucleation by porous materials (Everett, 1961; Blachere and Young, 1972). Porous materials such as mesoporous silica, zeolites, porous silicon, porous glass, and carbon nanotubes have morphologies similar to those of soot particles.

20   Therefore, the PCF mechanism may be applicable to soot particles as well (Marcolli (2014, 2017); Wagner et al. (2016); Ullrich et al. (2017)).

The PCF mechanism proposes that empty spaces between aggregated primary particles fill with water due to capillary forces and freeze homogeneously (that is liquid to solid transition) at relative humidity (RH_w) below water saturation in accord with the inverse Kelvin equation (Marcolli, 2014). The diameter of the pore affects the condensation process.

25   In large diameter pores, the water vapor pressure is not sufficient to cause condensation below water saturation (< 100 % RH_w). On the other hand, in pores with diameters too small, the growth of an ice embryo may be inhibited (Vali et al., 2015). Pore diameters in soot materials are typically on the order of nanometers and are dependent on the specific soot material. All else being equal, IN activity of a material is expected to increase with increasing number of pores in the suitable diameter range. The PCF mechanism also predicts the observed decrease in ice nucleation activity with

30   increasing temperature over the temperature range about 210 K to 240K (typical of cirrus clouds) (Hoose and Möhler, 2012).

Soot particles are emitted directly into the atmosphere from combustion processes such as agricultural burning, forest fires, domestic heating and cooking, and transportation (McCluskey et al., 2014; Arora & Jain, 2015; Vu et al., 2015; Sakamoto et al., 2016) and are ubiquitous in the Earth's troposphere (Heintzenberg, 1989; Seinfeld and Pandis, 1998;

35   Pósfai et al., 1999; Finlayson-Pitts and Pitts, 2000; Murphy et al., 2006). The chemistry and structure of soot depends on the type of fuel, combustion temperature, combustion kinetics and chemistry (Marcolli et al., 2014 and references therein; Murr and Soto, 2005). In general, soot particles consist primarily of elemental carbon with a chain-like

structure of aggregated primary spherules, which are typically tens of nanometers in diameter (Buseck et al., 2014). The size or mass of a soot particle depends upon the number of primary spheres and their arrangement as chain-like aggregates and agglomerates of aggregates, as illustrated schematically in Figure 1a. Electron-microscope images of an aggregate and a compact agglomerate of ethylene combustion soot are shown in Figs. 1b and 1c, respectively. In

5 the images, underlying the soot, is the substrate, on which the soot is collected.

The compact agglomerate structures contain pores. The edges of the agglomerate might have some external branched aggregates (Fig. 1c) that do not contribute to the porous structure. In this study we will refer to any confined empty spaces between aggregates as pores. Note that in this view, pores can occur both within and on the surface of the particle.

10 The critical factors that make some BC aerosols effective IN agents have not been established thus far. To elucidate these issues, we measured the ice nucleation properties for a series of five well-characterized commercial carbon black samples (proxies of BC) with varying morphologies and surface chemistries, as well as for ethylene flame-generated combustion soot. The studies were performed under systematically varied temperature in the range 217 – 235 K, simulating cirrus cloud-forming conditions (Krämer et al., 2016). In this connection, we studied the following factors

15 on soot particle ice nucleation activity:

(1) **Effect of particle morphology.** In the PCF mechanism, the dimensions and shape of the pores play an important role (Marcolli, 2017). In BC particles, it is not clear whether the PCF mechanism occurs in the empty spaces between primary spherules or in the pores formed between the aggregates (see Fig. 1). Therefore, spherule size, the degree of branching in a single aggregate, the stereo arrangement of the aggregates, and the location of the

20 pores may affect the IN activity of particles with similar mobility diameter. We studied the change in IN activity in agglomerates of the same selected mobility diameter but different internal spatial configuration of aggregates of spherules.

(2) **Effect of particle generation.** A question has been raised whether water processing of soot in the atmosphere and in the laboratory reduces the IN activity of soot. A possible explanation to the IN activity discrepancies

25 observed in past laboratory studies of BC particles were ascribed to the technique of aerosol generation. The technique of aerosol generation can often affect the morphology of the particle through a compaction mechanism (China et al., 2015a), which can then change the density and therefore affect the IN activity of the particle. Some laboratory studies (e.g. Ma et al., 2013; Friedbacher et al., 1999) showed that a water droplet that encloses an aggregate followed by subsequent water evaporation in the diffusion dryer will lead to the collapse of the soot

30 structure driven by the water surface tension exerted on the aggregate core. However, this compaction from aqueous suspensions was observed only in the laboratory and only for aggregates of approximately 200 nm in diameter (e.g. Ma et al., 2013; Khalizov et al., 2013). Some suggest that it can occur also in the atmosphere (e.g. China et al., 2015b). We examined both dry and wet particle generation techniques.

(3) **Role of particle size.** To test the role of particle size in the IN process, we compared IN activity of large BC

35 agglomerates with inner pores between aggregates (Fig. 1c) to IN activity of smaller size selected aggregates (Fig. 1b) with similar chemistry and morphology but smaller number of pores.

(4) **The influence of surface oxidation.** The influence of surface oxidation on IN activity of BC is still unclear. Some studies (e.g. Koehler et al., 2009; Gorbunov et al., 2001; Marcolli 2014) suggested that heterogeneous ice nucleation is favored on oxidized hydrophilic soot. However, others (e.g. Whale et al., 2015; Lupi et al., 2014a, 2014b; Biggs et al., 2017) suggested that a lower degree of oxidation leads to enhanced ice nucleation efficiency.

5   Our experiments explore the effect of oxidized surfaces.

(5) **The effect of organic coating.** A higher organic carbon content has been observed in laboratory experiments to suppress ice nucleation on soot particles (e.g. Möhler et al., 2005; Crawford et al., 2011; Kärcher et al., 2007). However, for some types of soot such a suppression of IN activity by coating is insignificant while in others it is notable. On the other hand, some organic acids could enhance IN activity (Zobrist et al., 2006; Wang and Knopf,

10   2011). The coating material may first fill the pores, thus depending on the type, coating may bring about inhibition or enhancement of IN activity. A series of experiments performed with a range of coatings on BC particles, provides some clarification on the effect of organics on the IN activity of BC particles.

2 Experimental Method

2.1 Materials Studied

15   In the present experiments, the ice nucleation properties of the six types of BC-containing particles, listed in Table 1, were studied. The first five of these materials are commercial carbon black, a form of elemental carbon obtained from the incomplete combustion of organics (typically liquid hydrocarbons) under controlled conditions. The first four were supplied by Cabot Corporation, the fifth material, Raven 2500 Ultra, manufactured by Birla Carbon was chosen for its relatively large specific surface area (high BET) value. These uniform commercial powders with known physical

20   properties allow a systematic screening of selected particle properties important for ice nucleation in the deposition mode regime.

Sub-micron soot particles were produced by an inverted burner soot generator (Argonaut Scientific Corp.) through combustion of ethylene (C_2H_4). In the present study, we chose to maintain the flame at a low net fuel equivalence ratio of 0.017 to avoid the polydisperse size distribution mode shifting to larger sizes due to agglomeration and also to

25   avoid clogging of tubing by the soot. These particles were collected on a filter and reaerosolized for ice nucleation measurements (see Sect. 2.2.1).

The BET and OAN values shown in Table 1, were provided by the manufacturers. The BET test (Brunauer et al., 1938) measures the specific surface area of materials by determining gas adsorption (usually N_2). The BET value is affected by primary particle size. Higher BET is associated with smaller primary particle size, in this case spherules.

30   The Oil Absorption Number (OAN) is an international standard measurement for characterizing carbon black, obtained by a well-defined test ASTM D2414 (ASTM, 2017) consisting of adding oil to the carbon black sample. This parameter is associated with the degree of branching of the black carbon particle. Higher OAN corresponds to more highly branched particle structures.

The surface chemistry and hydrophilicity can affect the IN activity of a particle (e.g. Koehler et al., 2009). To test this

35   effect, we included the surface oxidized Regal 400R carbon black pigment in this study, which was oxidized by the

manufacturer in a post combustion process. In order to test the acidity and solubility of surface groups on BC, we measured the pH of aqueous BC suspensions. We used an ultrasonic homogenizer and a sympHony B10P pH meter (VWR Scientific). The pH measurements confirmed the surface chemistries indicated by the manufacturers, with the Regal 400R carbon black samples exhibiting an acidic suspension, whereas the other samples all generated near neutral

5   suspensions (Table 1). In situ characterization measurements are described in the following sections.

2.2 Experimental Setup

2.2.1 Aerosol generation and characterization

A schematic diagram for the experimental apparatus is shown in Figure 2. The table inserted in the figure provides the code to instrument abbreviations. The BC particles which are in the form of a powder under dry conditions are

10   dispersed into a free-flowing dry nitrogen gas using a novel printed fluidized bed generator with an acronym PRIZE (Roesch et al., 2017). In addition to dry dispersion via the fluidized bed, samples were also atomized from an aqueous suspension with a 3-Jet Collison Nebulizer (BGI) to assess the impact of aerosol generation techniques on IN measurements ("issue 2" in the Introduction). The atomized BC particles were dried inline in a diffusion dryer (Topas DDU 570/H) filled with silica gel. Next, to study the effect of size and structure as discussed in "issues 1 – 3" outlined

15   in the Introduction, we selected particles of two mobility diameters (D_m), 100 and 800 nm. The size was selected by a Differential Mobility Analyzer (DMA, Brechtel) and counted by a mixing condensation particle counter (MCPC 1710, Brechtel).

In a study of the effect of organic carbon content on IN ("issue 5" in the Introduction), BC particles were coated either with stearic acid (SA) (>99 % purity, Aldrich), cis-pinonic acid (98 % purity, Aldrich), or oxalic acid (>99 % purity,

20   Aldrich). Size-selected BC particles were passed at a flow rate of 1.3 L min^{-1} through a heated temperature-controlled reservoir that contained the coating substance (Fig. 2). Temperatures during the coating process were adjusted for each organic material, and kept below the homogenous nucleation point of the coating substance. At temperatures below 200 K, the morphology of the BC aerosol would not change significantly (Bhandari et al., 2017). The phase and the thickness of the coating material was not directly determined in these experiments. At the temperature and

25   relative humidity conditions of the ice nucleation experiments, coatings consisting of super-cooled aqueous solutions, as well as crystalline or glassy solids, can form (Hearn and Smith, 2005; Knopf, 2018).

2.2.2 BC particle characterization

The DMA-selected BC particles were characterized for chemical composition by the Particle Analysis by Laser Mass Spectrometry (PALMS) instrument, described in detail by Cziczo et al., (2006) and Zawadowicz et al., (2015). Briefly,

30   particles are collimated in an aerodynamic inlet and pass through two 532 nm Nd:YAG laser beams. The time difference between scattering signals corresponds to particle velocity, which can be converted to vacuum aerodynamic diameter. Particles are then ionized using a 193 nm excimer laser. Either positive or negative ions can be detected. Particle vacuum aerodynamic diameter and chemical composition are measured in situ and in real time at the single-particle level. Due to highly variable ionization efficiencies and matrix effects of common atmospheric materials and

mixtures, single particle instruments such as PALMS are not considered quantitative. Hundreds of single particle spectra are acquired to compare relative compositions between similar samples.

In addition, BC particles of 800 nm mobility diameter were collected on copper grids and analyzed offline in a scanning electron microscope (Hitachi S-4700 FE-SEM). While BC aggregates are often branched (Fig. 1a), the

5   microscopic images of the collected agglomerates show that the aggregates have clustered in a spheroidal porous structure (Figs. 1c, A2). These images enable us to estimate the effective surface area based on single spherule size calculations. The surface area is then used together with the frozen fraction to calculate the density of the active sites (Vali et al., 2015). The active site density, $n_s(T)$, is defined as

$$n_s = \frac{A_f(T) \cdot L_f}{S_{eff}} \ [m^{-2}], \tag{1}$$

10   where $A_f(T)$ is the activated fraction at a given temperature, L_f is a correction factor obtained in flow calibrations, and S_{eff} is the effective surface area, which is calculated from the sum of the areas of spherules that form the outer shells of a BC particle of a given geometric volume. We assume that the geometric volume of the spheroidal agglomerates is comparable with the volume derived from the selected mobility diameter. This assumption may introduce an uncertainty factor of 3 due to the uncertainty in the number of outer layers that contribute to the total surface area. The

15   active site density analysis of the 800 nm particles enables us to study the effect of complex agglomerate structures on the IN activity (see Results Section).

2.3 Ice nucleation measurements

The ice nucleation measurement technique utilized here (blue dashed frame, Fig. 2), including the operation of the SPectrometer for Ice Nuclei (SPIN, Droplet measurement Technologies), calibration of the laminar flow fraction, and

20   the minimization of uncertainty of IN measurements is described in detail elsewhere (i.e. Garimella et al., 2016, 2017). Here, we describe only briefly the experimental steps. The SPIN instrument is a continuous flow diffusion chamber consisting of two flat, parallel aluminum plates, cooled independently to create a temperature gradient. The plates are covered with a layer of ice and due to the difference in their temperature, a linear gradient in water vapor partial pressure and temperature is set up between the two plates. Because of the nonlinear relationship between saturation

25   vapor pressure and temperature, supersaturation with respect to ice, in water subsaturation conditions, is achieved along the center of the chamber, allowing for heterogeneous ice nucleation in the deposition mode regime.

The laminar flow in the chamber can reach temperatures as low as 213 K, with a fixed particle residence time of approximately 10 s inside the chamber, at a sample flow rate of approximately 1 L min^{-1} such that nucleated ice crystals are able to grow to sizes of several micrometers. In each experiment, the average temperature of the laminar

30   flow was held constant while the relative humidity was slowly increased from subsaturated to supersaturated conditions with respect to ice and constantly subsaturated conditions with respect to water. We investigated BC heterogeneous ice nucleation activity at temperatures of 217 to 235 K and relative humidity with respect to ice (RH_i) between 100 and 150 %, typical to cirrus clouds.

Aerosol particles fed into the SPIN nucleation chamber in a lamina sample flow are nominally constrained to the

35   centerline with a sheath flow of about 9.0 L min^{-1}. However, turbulence at the inlet causes a fraction of particles to spread outside the centerline, decreasing the RH_i they are exposed to. As these particles are less likely to activate as

IN, a correction factor (5.8) is applied to fractional activation data obtained from the machine learning algorithm. Depending on experimental conditions, correction factors between 1.86 and 7.96 have been previously reported (Garimella et al. 2017; Wolf et al., 2018).

Nucleated ice crystals are detected in the SPIN by an optical particle counter (OPC, Droplet Measurement
5   Technologies) at the chamber outlet. The OPC measures particles from 500 nm to 15 µm diameter and has the ability to discriminate the phase of the particle by the 3 detected polarization components in 2 scattering angles using machine learning algorithms developed by Garimella et al. (2016). Ice formation onset is reported as the RH_i at which ice particles are identified by the machine learning algorithm.

Ice onset point is defined as the combination of supersaturation with respect to ice and temperature at which the
10   activated fraction threshold is reached. The activated fraction is defined as the number concentration of aerosol that are activated to form ice crystals detected by the OPC divided by the total number concentration, counted by MCPC (Fig. 2). This activation threshold does not have a universally agreed value (Kanji et al., 2017). In our study, we have set it at 1 %.

3 Results and discussion

15   **3.1 Ice onset**

The ice onset points for 800 nm particles, together with experimental error bars, are presented in Figure 3. This figure shows a plot of water vapor supersaturation ratio over ice versus temperature at which (1 %) ice onset occurs. This time dependent approach is based on kinetics in the ~10 s period of particle passing through the chamber and the set supersaturation conditions. The most obvious aspect of these results is the bifurcation in the ice onset measurements
20   with decreasing temperatures. The Regal 400R results remain indistinguishable from the homogeneous ice nucleation line, whereas the other BC particle types all exhibit decreasing ice onsets with decreasing temperatures. For a given temperature, the lower the supersaturation at the onset of ice nucleation, the greater is the effectiveness of the particle as an IN agent.

Measurements of IN activity for non-oxidized commercial carbon-black particles show the same trend in IN activity
25   of soot collected from ethylene combustion. Both types demonstrated temperature dependence of ice onset similar to some of the earlier observations of soot (e.g. Ullrich et al., 2017; Bond et al., 2013), associated with the PCF mechanism, that is, increasing ice onset point with increasing temperature in the range 217 – 235 K.

Heterogeneous ice nucleation was observed for the non-oxidized BC proxies and soot with identical mobility diameter of 800 nm. As is evident, the data differ for each sample. To understand these differences and to simplify the
30   discussion, we will address each issue outlined in the introduction, separately.

We extracted and replotted salient data from Figure 3 related to the specific issues and display them in Figures 4 to 7. These figures provide significant information related to issues 1 to 4 outlined in the Introduction. The color-coded solid lines in Fig. 4 are guides to the eye. An additional set of measurements was obtained for the 100 nm particles. Those results are presented in Figure 6.

(1) Effect of particle morphology: The most notable feature in Figure 4 is the gradient between the guiding lines for BC particles Raven 2500Ultra (R2500U) (red squares) and Regal 330R (yellow squares), including the BC types in between. The displayed onset supersaturation difference shows that the IN activity of R2500U is significantly higher than that of Regal 330R. This is most likely due to the difference in the BET parameters for the two species; for

5 R2500U BET = 270 $m^2\ g^{-1}$ and for Regal 330R BET = 90 $m^2\ g^{-1}$. As stated in Sect. 2.1, higher BET values correlate with higher surface areas, typically implying smaller primary particle size. In turn smaller spherules tend to lead to higher branching within the BC material and hence a greater number of pores. Chughtai et al. (1999) showed that larger surface area of carbonaceous material determines the adsorption capacity of water molecules at high RH. Other studies demonstrated ice formation in hydrophobic confinements (e.g. Bampoulis et al., 2016; Bi et al., 2017; Zhu et

10 al., 2018). Therefore, a higher number of smaller pores in BC particles may facilitate condensation of water in sub-saturated conditions and subsequent freezing in ice super-saturated conditions. In accord with the PCF mechanism, higher number of pores is associated with greater IN activity as is consistent in our results.

A hint for the subtle influence of aggregate branching on IN activity can be found in the comparison of Monarch 880 (grey squares), Monarch 900 (blue squares), and R2500U (red squares) (Fig. 4), all have nearly the same specific

15 surface area (Table 1), while the OAN number, which is a measure of branching, is higher for Monarch 880 by 60 %. Higher branching may contribute to less compact structure and larger diameter pores that display a weaker Kelvin effect with the consequent reduction in the propensity of water to condense in them and freeze as readily. Therefore, in accord with the PCF mechanism, one would expect Monarch 880 to display lower IN activity in comparison to Monarch 900 and R2500U, as is observed.

20 The dimensions of the pores in the BC agglomerate, that is, the density of the BC agglomerate, in this case, is primarily governed by the entangled contribution of the single spherule size and the degree of branching of the enclosed aggregate. For a constant selected mobility diameter of 800 nm, we observed variability in the effective density derived from the ratio of the vacuum aerodynamic diameter measured by the PALMS instrument for each BC sample and the mobility diameter (DeCarlo et al., 2004) (Table 1). The aerodynamic diameter of the agglomerates is related to their

25 mass, and the shape factor (DeCarlo et al., 2004; Jayne et al., 2000). A similar round shape of agglomerates was observed for numerous BC samples in the electron microscope (Fig. A2). The variability in IN activity of particles that have the same mobility diameter and chemical composition (Fig. 4) can be explained by the variability in particle effective density (i.e. pore number concentration and dimensions). The more effective INP have a higher effective density (i.e., more compact particle) with a higher density of IN pores. While the lacy BC with low effective density

30 will have fewer IN pores.

Another method for physical characterization is the detection of the shift in polarization in the light scattered from 800 nm BC particles in the OPC. The optical sphericity could shed light on the BC particle shape (i.e. round and compact versus branched and lacy) and its influence on the IN mechanism in BC agglomerates. High optical sphericity of a particle is determined by a low polarization shift in the light scattered from the particle. OPC data cluster centers

35 of single-particle optical measurements for each BC sample are listed in Table 1. In our experiments, the most active INP (e.g. R2500U, Monarch 900) showed lower polarization shift signatures, which suggests a more optically spherical shape.

Atmospheric
Chemistry
and Physics
Discussions

(2) Effect of particle generation: In order to test the effect of aerosol generation technique on IN measurements, we measured the IN activity of BC atomized from a liquid suspension and dried in a diffusion dryer in comparison with IN activity of the same BC dry-aerosolized. The results showed no visible sign of compaction effects on IN activity of 800 nm BC particles (Fig. 5). The dry-aerosolized round compact shapes observed in Fig. A2 may explain the lack

5 of further compaction during the atomization process of 800 nm BC aerosol. Further qualitative support for the hypothesis of initial compactness of the particles was provided by the low values measured in the OPC (Table 1), which are associated with the sphericity of the particles.

(3) Role of particle size: To test the extremes of the aerosol diameters used in previous studies we selected 100 nm and 800 nm BC particles. The results of experiments shown in Figure 6 demonstrate the influence of the BC particle

10 size on its IN activity. The smaller mobility diameters of 100 nm, which are likely to be single aggregates (Fig. 1b), do not nucleate as readily as the larger agglomerates of 800 nm of the same composition, spherule size, and branching, The BC particles are hydrophobic and non-crystalline with particle size-independent packing density as shown in Zangmeister et al. (2014), therefore, according to the stochastic approach, an increase of the surface area should not affect their IN activity, however according to singular approach, the number of active sites will be higher on a bigger

15 surface area, increasing the probability to nucleate. Hence, the enhancement of the IN activity in each 800 nm BC sample shown in Fig. 6 suggests a unique structural change as the mobility diameter is increased. It is plausible that these particles nucleate via the PCF mechanism by capillary condensation in empty spaces between soot aggregates due to the inverse Kelvin effect. The number of aggregates that form the agglomerate define the number and the dimensions of pores that act as IN, which in the extreme case of single aggregate (i.e. without suitable pores) nucleate

20 homogeneously (e.g. grey circles in Fig. 6). The IN activity of 100 nm ethylene flame soot is reduced in comparison to the 800 nm soot. Despite the reduction in activity, the 100 nm soot has nucleated ice heterogeneously. It is possible that a bias introduced by doubly charged particles, passed at the same DMA voltage, maintained the high IN activity of 100 nm soot.

(4) The influence of surface oxidation: In Figure 7, the oxidized sample of Regal 400R (green) is compared to a

25 similar non-oxidized sample of Regal 330R (yellow). In addition to pH values (Table 1) obtained for each suspension of BC samples, we used the PALMS instrument to confirm the oxidation state of dry particles. Negative and positive ion spectra of about 1000 particles were collected for each BC sample. The oxygen negative ion peaks were then plotted against carbon negative ion peaks and color-coded for each BC sample (Fig. A1). Regal 400R particles cluster demonstrates noticeably higher peaks of oxygen in comparison to other BC samples. This oxidized sample froze

30 homogeneously even at temperatures as low as 219 K while the non-oxidized sample showed heterogeneous nucleation activity. This observation is initially counterintuitive due to the presumed hydrophilicity of the oxidized sample, however the ubiquity of oxygenated surface groups on BC surfaces does not mean that soot particles will appear hydrophilic on a macroscopic scale. For example, fresh, oxidized soot particles do not generally activate as cloud-condensation nuclei (CCN) under atmospherically relevant conditions (Corbin et al., 2015). Moreover,

35 molecular dynamics calculations show that hydrophilicity is not a sufficient condition for IN (Lupi et al., 2014a, 2014b). In fact, Biggs et al. (2017) reported an increase in the ice nucleation activity due to a decrease in hydrophilicity.

The freezing behavior of water confined in pores of an oxidized BC sample is not affected by pore wall hydrophobicity or hydrophilicity (Morishige, 2018). Häusler et al. (2018) suggested that agglomeration may lead to a favorable positioning of the functional sites and therefore to an increase in the IN activity, even though a decrease in the surface area occurs. However, it was found that the increased proportion of oxygen increases the hydrophilicity of graphene, reduces agglomeration and hence increases the surface area and reduces the number of pores (Häusler et al., 2018). Our observations of homogeneous ice nucleation by the oxidized BC sample suggest that the surface oxidation of BC blocks pore-induced-freezing possibly due to the exceedingly high polarity of the surface, which consequently imposes dipole orientation that raises the free energy of formation of ice embryos (Fletcher, 1959). In other words a restriction of access of water molecules into the pores where they can condense and freeze. This might also explain the surprisingly high effective density of Regal 400R sample, possibly due to a water layer formation on the oxidized surface even in dry aerosolization.

The combined contribution of single spherule size, particle size, surface oxidation, and morphology to IN activity affects the spatial arrangement and thus the adjacent angles in the pores that dictate the formation, and perhaps the type, of the ice lattice (Bi et al., 2017; Zhu et al., 2018). However, further screening of BC samples accompanied by thorough characterization is needed to confirm these findings.

 (5) The effect of organic coating: Surface oxidation is not the only process altering the IN activity. Previous studies have shown that a higher organic carbon content significantly suppresses ice nucleation on soot particles (e.g. Möhler et al., 2005; Kärcher et al., 2007). Crawford et al. (2011) showed that alteration of the organic carbon content from minimum (5 %) to medium (30 %) results in a clear transition between heterogeneous and homogeneous freezing mechanism, respectively. However, for some types of BC such a suppression of IN activity by a coating is insignificant while in others it is prominent. On the other hand, some organic acids enhance IN activity (Zobrist et al., 2006; Wang and Knopf, 2011). Coating material may fill the pores, and the extent of inhibition or enhancement of IN activity may imply the prevalent ice formation mechanism for BC agglomerates. The cis-pinonic and stearic acid when atomized, nucleate ice homogeneously. When used as coatings they decreased the IN activity of R2500U (Fig. 8b, c). The pure atomized oxalic acid on the other hand, nucleates ice heterogeneously at supersaturation as low as 10 %. When used as a coating material, it has increased the IN activity of a homogeneously nucleating BC sample, Regal 400R, to ~30 % superstation at ice onset (Fig. 8a).

3.2 Active site density

As we mentioned in the introduction, two approaches to explain the IN data are commonly used: a stochastic description based on classical nucleation theory and a deterministic or singular description (Knopf et al, 2018). The time-independent, singular approach is often used in models where a surface density of sites active on a particle surface (Eq. 1) can initiate ice nucleation at a given temperature, assuming that one site gives rise to a single ice crystal.

 The ice onset points for 800 nm particles are presented in Figure 9. Shown in the figure as black dashed lines, are active site density isolines (10^{10} m^{-2}, 10^{11} m^{-2} and 10^{12} m^{-2}) derived from empirical parametrization of ice nucleation

on soot from five sources by Ullrich et al. (2017). IN activity of non-oxidized particles, as measured in this study, lies mostly within the boundaries confined by the 10^{10} and 10^{11} m^{-2} active site density isolines.

In our study to calculate the active site density, we use the activated fraction of aerosol derived from OPC and MCPC measurements divided by the effective surface area of the BC particle. We use the single spherule diameter measured

5 in the electron microscope images of 800 nm BC particles to estimate the effective surface area of the spheroidal compacted shapes of agglomerates with defined mobility diameter (Eq. 1).

In Figure 10, the calculated active site densities of the most active BC proxies, at the lowest measured temperatures, complement the data reproduced from Kanji et al. (2017). The calculated n_s appear in the same range of 10^{10} and 10^{11} m^{-2}, in agreement with the parametrization by Ullrich et al. (2017). The uncertainties in effective surface area

10 calculations together with activated fraction uncertainties are propagated to a total uncertainty of less than an order of magnitude.

4 Atmospheric implications

Previous laboratory studies of ice nucleation by carbonaceous particles in the cirrus cloud regime revealed widespread in IN activity (e.g. Kulkarni et al. (2016); Friedman et al. (2011); China et al. (2015a); Ullrich et al. (2017); Cziczo

15 et al. (2016); Demott et al. (2009); Kanji et al. (2017); Hoose and Möhler, (2012)), which obscures understanding of the radiative properties of clouds and Earth's climate. Our findings show that large agglomerates, such as observed in wild fires (Chakrabarty et al., 2014), could be a potential source of efficient heterogeneous IN via the PCF mechanism in cirrus cloud conditions in the troposphere. While the concentration of such large particle is usually low, hindering their detection, these efficient INP may contribute to the warming effect. Bond et al., 2013 modelled the contribution

20 of soot to clouds and climate and distinguished between the homogeneous and heterogeneous nucleation types. They showed that in the case of ice clouds when homogeneous nucleation dominates, high clouds coverage is reduced and cooling prevails while when heterogeneous nucleation of BC prevails, more high clouds are formed that in turn contribute indirectly to the warming effect. Our study explained some of the main factors that affect the high variability in IN activity of different BC, which can shift between heterogeneous and homogeneous ice nucleation. For

25 comparable oxidized and non-oxidized particles, several orders of magnitude differences in active sites density were observed. Organic coatings not only cover the outer layers of BC aggregates but may also fill the internal pores among primary spherules and have the ability to both inhibit or enhance IN activity. Hence, the singular, time independent, parametrization approach in models should take into account the oxidation state and coating of the BC particles.

We showed that our results of heterogeneous ice nucleation on BC particles are consistent with the PCF mechanism.

30 However, these findings seem to contradict some field observations, where no clear evidence of heterogeneous IN activity of BC was found (see Introduction Section). Such contradictory observations between laboratory and field measurements can be explained by ice multiplication processes (e.g. Ladino et al., 2017), as well as, decrease of IN activity by surface coatings (Friedman et al., 2011), instrumental limitations (Cziczo et al., 2014), and scarcity of data from field measurements. If PCF is to occur in atmospheric BC particles, less studied mechanisms of ice

35 multiplication, resembling supercooled droplet splintering upon freezing (Wildeman et al., 2017), may occur during

Atmospheric
Chemistry
and Physics
Discussions

pore condensation and freezing, inside the confined geometry (Vlahou and Worster, 2010; Kyakuno et al., 2010; Kyakuno et al., 2016), which is sensitive to surface coatings. This in turn could be another plausible explanation to the scarcity of BC in ice residuals collected in field measurements and the reason for the underestimation of BC IN activity and its global IN importance.

5 Conclusions

In this study, we systematically examined the ice nucleating activity of well-characterized commercial carbon black samples and soot generated in an inverted diffusion flame. A commercial continuous flow diffusion chamber (SPIN) was used to simulate the temperature and humidity conditions of the in situ type cirrus clouds (Krämer et al., 2016). Our results complement the ongoing research of IN activity of BC aerosol in atmospherically relevant simulated conditions. The majority of BC samples tested here showed IN activity at low supersaturation over ice with a strong dependence on the temperature, in agreement with previous reported results. Our data suggests that the main IN mechanism in the majority of the particles tested is consistent with pore condensation and freezing, which occurs in empty spaces between the aggregates. Our main observations are listed below:

- Differences in the morphology of the agglomerate corresponded with differences in IN activity. Particles of the same diameter, with higher specific surface area and lower branching showed the highest IN activity.
- Aerosol generation techniques (i.e. dry versus wet-dried), and compaction, previously reported for ~200 nm BC, did not seem to have a significant effect on the IN activity of atomized 800 nm agglomerates.
- While comparing particle size (i.e. agglomerate versus aggregate), we observed a significantly lower IN activity at 100 nm mobility diameter versus 800 nm.
- Oxidized particles nucleated homogeneously for all tested temperatures.
- Organic surface coatings demonstrated the capability of both enhancing and inhibiting the IN activity on BC proxies.

Our study indicates that ice nucleation activity of commercial carbon black can be enhanced over homogeneous freezing. One can select a well-defined morphology of compact, non-oxidized agglomerates with high BET and low OAN values, which correspond to smaller spherules and low branching, respectively. Such a material will allow controlled conditions for more efficient ice nucleation. In future studies, IN activity enhancement with size should be tested in more detail, in the range 100 – 800 nm. This enhancement in non-oxidized, compact agglomerates of commercial carbon black should be similarly tested with other compounds of comparable morphology to understand the impact of the PCF mechanism on atmospheric processes.

6 Appendix A.

7 Author contribution

LN designed the experiments and LN, MF, YZ carried them out. PD, TO, DW, DC, CM supervised and administrated the project, acquired funding, and provided resources and facilities to conduct the experiments. MF processed the ice

nucleation data. JB processed the SEM data. LN, PD, TO prepared the manuscript with contributions from all co-authors.

References

ASTM D2414-17, Standard Test Method for Carbon Black—Oil Absorption Number (OAN), ASTM International, West Conshohocken, PA, 2017, www.astm.org

Arora, P. and Jain, S.: Morphological characteristics of particles emitted from combustion of different fuels in improved and traditional cookstoves, J. Aerosol Sci., 82, 13–23, doi:10.1016/j.jaerosci.2014.12.006, 2015.

Bampoulis, P., Teernstra, V. J., Lohse, D., Zandvliet, H. J. W. and Poelsema, B.: Hydrophobic ice confined between graphene and MoS2, J. Phys. Chem. C, 120(47), 27079–27084, doi:10.1021/acs.jpcc.6b09812, 2016.

Bhandari, J., China, S., Onasch, T., Wolff, L., Lambe, A., Davidovits, P., Cross, E., Ahern, A., Olfert, J., Dubey, M. and Mazzoleni, C.: Effect of Thermodenuding on the Structure of Nascent Flame Soot Aggregates, Atmos., 8(9), doi:10.3390/atmos8090166, 2017.

Bi, Y., Cao, B. and Li, T.: Enhanced heterogeneous ice nucleation by special surface geometry, Nat. Commun., 8(May), 15372, doi:10.1038/ncomms15372, 2017.

Biggs, C. I., Packer, C., Hindmarsh, S., Walker, M., Wilson, N. R., Rourke, P. and Gibson, M. I.: Impact of sequential surface-modification of graphene oxide on ice nucleation †, Phys. Chem. Chem. Phys., 19, 21929–21932, doi:10.1039/C7CP03219F, 2017.

Blachere, J. R. and Young, J. E.: The Freezing Point of Water in Porous Glass, J. Am. Ceram. Soc., 55(6), 306–308, doi:10.1111/j.1151-2916.1972.tb11291.x, 1972.

Bond, T. C., Doherty, S. J., Fahey, D. W., Forster, P. M., Berntsen, T., Deangelo, B. J., Flanner, M. G., Ghan, S., Kärcher, B., Koch, D., Kinne, S., Kondo, Y., Quinn, P. K., Sarofim, M. C., Schultz, M. G., Schulz, M., Venkataraman, C., Zhang, H., Zhang, S., Bellouin, N., Guttikunda, S. K., Hopke, P. K., Jacobson, M. Z., Kaiser, J. W., Klimont, Z., Lohmann, U., Schwarz, J. P., Shindell, D., Storelvmo, T., Warren, S. G. and Zender, C. S.: Bounding the role of black carbon in the climate system: A scientific assessment, J. Geophys. Res. Atmos., 118(11), doi:10.1002/jgrd.50171, 2013.

Brunauer, S., Emmett, P. H., and Teller, E.: Adsorption of gases in multimolecular layers, J. Am. Chem. Soc., 60, 309–319, 1938.

Buseck, P. R., Adachi, K., Gelencsér, A., Tompa, É. and Pósfai, M.: Ns-Soot: A Material-Based Term for Strongly Light-Absorbing Carbonaceous Particles, Aerosol Sci. Technol., 48(7), 777–788, doi:10.1080/02786826.2014.919374, 2014.

Campbell, J. M., Meldrum, F. C. and Christenson, H. K.: Observing the formation of ice and organic crystals in active
5   sites, Proc. Natl. Acad. Sci., 114(5), 810–815, doi:10.1073/pnas.1617717114, 2017.

Chakrabarty, R. K., Beres, N. D., Moosmüller, H., China, S., Mazzoleni, C., Dubey, M. K., Liu, L. and Mishchenko, M. I.: Soot superaggregates from flaming wildfires and their direct radiative forcing, Sci. Rep., 4, 1–9, doi:10.1038/srep05508, 2014.

Chen, J., Wu, Z., Augustin-Bauditz, S., Grawe, S., Hartmann, M., Pei, X., Liu, Z., Ji, D., and Wex, H.: Ice-nucleating
10   particle concentrations unaffected by urban air pollution in Beijing, China, Atmos. Chem. Phys., 18, 3523-3539, https://doi.org/10.5194/acp-18-3523-2018, 2018.

China, S., Kulkarni, G., Scarnato, B. V., Sharma, N., Pekour, M., Shilling, J. E., Wilson, J., Zelenyuk, A., Chand, D., Liu, S., Aiken, A. C., Dubey, M., Laskin, A., Zaveri, R. A. and Mazzoleni, C.: Morphology of diesel soot residuals from supercooled water droplets and ice crystals: Implications for optical properties, Environ. Res. Lett.,
15   doi:10.1088/1748-9326/10/11/114010, 2015a.

China, S., Scarnato, B., Owen, R. C., Zhang, B., Ampadu, M. T., Kumar, S., Dzepina, K., Dziobak, M. P., Fialho, P., Perlinger, J. A., Hueber, J., Helmig, D., Mazzoleni, L. R. and Mazzoleni, C.: Morphology and mixing state of aged soot particles at a remote marine free troposphere site: Implications for optical properties, Geophys. Res. Lett., 42(4), 1243–1250, doi:10.1002/2014GL062404, 2015b.

20   Chughtai, A. R., Williams, G. R., Atteya, M. M. O., Miller, N. J. and Smith, D. M.: Carbonaceous particle hydration, Atmos. Environ., 33(17), 2679–2687, doi:10.1016/S1352-2310(98)00329-X, 1999.

Corbin, J. C., Lohmann, U., Sierau, B., Keller, A., Burtscher, H. and Mensah, A. A.: Black carbon surface oxidation and organic composition of beech-wood soot aerosols, Atmos. Chem. Phys., 15(20), 11885–11907, doi:10.5194/acp-15-11885-2015, 2015.

25   Crawford, I., Möhler, O., Schnaiter, M., Saathoff, H., Liu, D., McMeeking, G., Linke, C., Flynn, M., Bower, K. N., Connolly, P. J., Gallagher, M. W. and Coe, H.: Studies of propane flame soot acting as heterogeneous ice nuclei in conjunction with single particle soot photometer measurements, Atmos. Chem. Phys., 11(18), 9549–9561, doi:10.5194/acp-11-9549-2011, 2011.

Cziczo, D. J. and Froyd, K. D.: Sampling the composition of cirrus ice residuals, Atmos. Res., 142, 15–31,
30   doi:10.1016/j.atmosres.2013.06.012, 2014.

Cziczo, D. J., Thomson, D. S., Thompson, T. L., DeMott, P. J. and Murphy, D. M.: Particle analysis by laser mass spectrometry (PALMS) studies of ice nuclei and other low number density particles, Int. J. Mass Spectrom., 258(1–3), 21–29, doi:10.1016/j.ijms.2006.05.013, 2006.

Cziczo, D., Ladino-Moreno, L., Boose, Y., Kanji, Z., Kupiszewski, P., Lance, S., Mertes, S. and Wex, H.:
35   Measurements of Ice Nucleating Particles and Ice Residuals, Meteor. Monogr, (April), doi:10.1175/AMSMONOGRAPHS-D-16-0008.1, doi:10.1175/AMSMONOGRAPHS-D-16-0008.1, 2016.

Decarlo, Peter F., Slowik, J. G., Stainken, K., Davidovits, P., Williams, L. R., Jayne, J. T., Kolb, C. E., Worsnop, D. R., Rudich, Y., DeCarlo, P. F. and Jimenez, J. L.: Particle morphology and density characterization by combined mobility and aerodynamic diameter measurements. Part 2: Application to combustion-generated soot aerosols as a function of fuel equivalence ratio, Aerosol Sci. Technol., 38(12), 1206–1222, doi:10.1080/027868290903916, 2004.

5 DeMott, P. J.: An Exploratory Study of Ice Nucleation by Soot Aerosols, J. Appl. Meteorol., 29(10), 1072–1079, doi:10.1175/1520-0450(1990)029<1072:AESOIN>2.0.CO;2, 1990.

DeMott, P. J., Chen, Y., Kreidenweis, S. M., Rogers, D. C., and Sherman, D. E.: Ice formation by black carbon particles, Geophys. Res. Lett., 26, 2429–2432, doi:10.1029/1999gl900580, 1999.

DeMott, P. J., Petters, M. D., Prenni, A. J., Carrico, C. M., Kreidenweis, S. M., Collett, J. L. and Moosmüller, H.: Ice
10 nucleation behavior of biomass combustion particles at cirrus temperatures, J. Geophys. Res. Atmos., 114(16), 1–13, doi:10.1029/2009JD012036, 2009.

Eriksen Hammer, S., Mertes, S., Schneider, J., Ebert, M., Kandler, K., and Weinbruch, S.: Composition of ice particle residuals in mixed phase clouds at Jungfraujoch (Switzerland): Enrichment and depletion of particle groups relative to total aerosol, Atmos. Chem. Phys. Discuss., https://doi.org/10.5194/acp-2018-478, in review, 2018.

15 Everett, D.H., The thermodynamics of frost damage to porous solids, Transactions of the Faraday Society, 57, 1541-1551, 1961.

Finlayson-Pitts, B. J., and J. N. Pitts Jr. (2000), Chemistry of the Upper and Lower Atmosphere, Elsevier, New York.

Fletcher, N. H.: Entropy Effect in Ice Crystal Nucleation, J. Chem. Phys., 30(6), 1476–1482, doi:10.1063/1.1730221, 1959.

20 Friedbacher, G., Kotzick, R., Niessner, R. and Grasserbauer, M.: In-situ atomic force microscopy investigation of aerosols exposed to different humidities, , 296–304, 1999.

Friedman, B., Kulkarni, G., Beránek, J., Zelenyuk, A., Thornton, J. A. and Cziczo, D. J.: Ice nucleation and droplet formation by bare and coated soot particles, J. Geophys. Res. Atmos., 116(17), 1–11, doi:10.1029/2011JD015999, 2011.

25 Garimella, S., Bjerring Kristensen, T., Ignatius, K., Welti, A., Voigtländer, J., Kulkarni, G. R., Sagan, F., Lee Kok, G., Dorsey, J., Nichman, L., Alexander Rothenberg, D., R??sch, M., Kirchgäßner, A. C. R., Ladkin, R., Wex, H., Wilson, T. W., Antonio Ladino, L., Abbatt, J. P. D., Stetzer, O., Lohmann, U., Stratmann, F. and James Cziczo, D.: The SPectrometer for Ice Nuclei (SPIN): An instrument to investigate ice nucleation, Atmos. Meas. Tech., 9(7), 2781–2795, doi:10.5194/amt-9-2781-2016, 2016.

30 Garimella, S., Rothenberg, D. A., Wolf, M. J., David, R. O., Kanji, Z. A., Wang, C., Roesch, M. and Cziczo, D. J.: Uncertainty in counting ice nucleating particles with continuous diffusion flow chambers, Atmos. Chem. Phys. Discuss., (January), 1–28, doi:10.5194/acp-2016-1180, 2017.

Gasser, T., Peters, G. P., Fuglestvedt, J. S., Collins, W. J., Shindell, D. T., and Ciais, P.: Accounting for the climate–carbon feedback in emission metrics, Earth Syst. Dynam., 8, 235-253, https://doi.org/10.5194/esd-8-235-2017, 2017.

35 Gorbunov, B., Baklanov, A., Kakutkina, N., Windsor, H. L., and Toumi, R.: Ice nucleation on soot particles, J. Aerosol Sci., 32, 199–215, doi:10.1016/S0021-8502(00)00077-X, 2001.

Häusler, T., Gebhardt, P., Iglesias, D., Rameshan, C., Marchesan, S., Eder, D. and Grothe, H.: Ice Nucleation Activity of Graphene and Graphene Oxides, J. Phys. Chem. C, 122(15), 8182–8190, doi:10.1021/acs.jpcc.7b10675, 2018.

Hearn, J. D., and G. D. Smith: Measuring rates of reaction in super- cooled organic particles with implications for atmospheric aerosol, Phys. Chem. Chem. Phys., 7, 2549–2551, doi:10.1039/b506424d, 2005.

5   Heintzenberg, J. (1989), Fine particles in the global troposphere A review. Tellus B, 41B: 149-160. doi:10.1111/j.1600-0889.1989.tb00132.x

Hoose, C. and Möhler, O.: Heterogeneous ice nucleation on atmospheric aerosols: a review of results from laboratory experiments, Atmos. Chem. Phys., 12, 9817-9854, https://doi.org/10.5194/acp-12-9817-2012, 2012.

Jayne, J. T., Leard, D. C., Zhang, X. F., Davidovits, P., Smith, K. A., Kolb, C. E., and Worsnop, D. R.: Development
10   of an Aerosol Mass Spectrom- eter for Size and Composition Analysis of Submicron Particles, Aerosol Sci. Technol. 33(1–2):49–70, 2000.

Jensen, E. J., and O. B. Toon: The potential impact of soot particles from aircraft exhaust on cirrus clouds, Geophys. Res. Lett., 24(3), 249–252, 1997.

Kanji, Z.A. and Abbatt P.D.: Laboratory studies of ice formation via deposition mode nucleation onto mineral dust
15   and n-hexane soot samples, J. Geophys. Res. Atmos., 111(D16), doi:10.1029/2005JD006766, 2006.

Kanji, Z. A., Ladino, L. A., Wex, H., Boose, Y., Burkert-Kohn, M., Cziczo, D. J. and Krämer, M.: Overview of Ice Nucleating Particles, Meteorol. Monogr., 58, 1.1-1.33, doi:10.1175/AMSMONOGRAPHS-D-16-0006.1, 2017.

Kärcher, B., Lohmann, U.: A parameterization of cirrus cloud formation: heterogeneous freezing. J. Geophys. Res. 108, 4402, 2003.

20   Kärcher, B., Möhler, O., DeMott, P. J., Pechtl, S., and Yu, F.: Insights into the role of soot aerosols in cirrus cloud formation, Atmos. Chem. Phys., 7, 4203-4227, https://doi.org/10.5194/acp-7-4203-2007, 2007.

Khalizov, A. F., Lin, Y., Qiu, C., Guo, S., Collins, D. and Zhang, R.: Role of OH-Initiated Oxidation of Isoprene in Aging of Combustion Soot, Environ. Sci. Technol., 47(5), 2254–2263, doi:10.1021/es3045339, 2013.

Kiselev, A., Bachmann, F., Pedevilla, P., Cox, S. J., Michaelides, A., Gerthsen, D. and Leisner, T.: Active sites in
25   heterogeneous ice nucleation—the example of K-rich feldspars, Science (80), 355(6323), 367–371, doi:10.1126/science.aai8034, 2017.

Knopf, D. A., Alpert, P. and Wang, B.: The Role of Organic Aerosol in Atmospheric Ice Nucleation – A Review, ACS Earth Sp. Chem., acsearthspacechem.7b00120, doi:10.1021/acsearthspacechem.7b00120, 2018.

Koehler: Cloud condensation nuclei and ice nucleation activity of hydrophobic and hydrophilic soot particles, Phys.
30   Chem. Chem. Phys., doi:10.1039/b905334b, 2009.

Koop, T., Luo, B. P., Tsias, A., and Peter, T.: Water activity as the determinant for homogeneous ice nucleation in aqueous so- lutions, Nature, 406, 611–614, 2000.

Krämer, M., Rolf, C., Luebke, A., Afchine, A., Spelten, N., Costa, A., Meyer, J., Zöger, M., Smith, J., Herman, R. L., Buchholz, B., Ebert, V., Baumgardner, D., Borrmann, S., Klingebiel, M., and Avallone, L.: A microphysics guide to
35   cirrus clouds – Part 1: Cirrus types, Atmos. Chem. Phys., 16, 3463-3483, https://doi.org/10.5194/acp-16-3463-2016, 2016.

Atmospheric
Chemistry
and Physics
Discussions

Open Access

EGU

Kulkarni, G., China, S., Liu, S., Nandasiri, M., Sharma, N., Wilson, J., Aiken, A. C., Chand, D., Laskin, A., Mazzoleni, C., Pekour, M., Shilling, J., Shutthanandan, V., Zelenyuk, A. and Zaveri, R. A.: Ice nucleation activity of diesel soot particles at cirrus relevant temperature conditions: Effects of hydration, secondary organics coating, soot morphology, and coagulation, Geophys. Res. Lett., 43(7), 3580–3588, doi:10.1002/2016GL068707, 2016.

5   Kyakuno, H., Fukasawa, M., Ichimura, R., Matsuda, K., Nakai, Y., Miyata, Y., Saito, T. and Maniwa, Y.: Diameter-dependent hydrophobicity in carbon nanotubes, J. Chem. Phys., 145(6), doi:10.1063/1.4960609, 2016.

Kyakuno, H., Matsuda, K., Yahiro, H., Fukuoka, T., Miyata, Y., Yanagi, K., Maniwa, Y., Kataura, H., Saito, T., Yumura, M. and Iijima, S.: Global Phase Diagram of Water Confined on the Nanometer Scale, J. Phys. Soc. Japan, 79(8), 83802, doi:10.1143/JPSJ.79.083802, 2010.

10   Ladino, L. A., A. Korolev, I. Heckman, M. Wolde, A. M. Fridlind, and A. S. Ackerman: On the role of ice-nucleating aerosol in the formation of ice particles in tropical mesoscale convective systems, Geophys. Res. Lett., 44, 1574–1582, doi: 10.1002/2016GL072455, 2017.

Lavanchy, V. M. H., H. W. Gaggeler, U. Schotterer, M. Schwikowski, and U. Baltensperger, Historical record of carbonaceous particle concentrations from a European high-alpine glacier (Colle Gnifetti, Switzerland), J. Geophys.

15   Res., 104(D17), 21,227–21,236, 1999.

Lee, D. S., Fahey, D. W., Forster, P. M., Newton, P. J., Wit, R. C. N., Lim, L. L., Owen, B. and Sausen, R.: Aviation and global climate change in the 21st century, Atmos. Environ., 43(22), 3520–3537, doi:https://doi.org/10.1016/j.atmosenv.2009.04.024, 2009.

Levin, E. J. T., Mcmeeking, G. R., Demott, P. J., Mccluskey, C. S., Stockwell, C. E., Yokelson, R. J. and Kreidenweis,

20   S. M.: A new method to determine the number concentrations of refractory black carbon ice nucleating particles, Aerosol Sci. Technol., 48(12), 1264–1275, doi:10.1080/02786826.2014.977843, 2014.

Long, C. M., Nascarella, M. A. and Valberg, P. A.: Carbon black vs. black carbon and other airborne materials containing elemental carbon: Physical and chemical distinctions, Environ. Pollut., 181, 271–286, doi:10.1016/j.envpol.2013.06.009, 2013.

25   Lupi, L. and Molinero, V.: Does Hydrophilicity of Carbon Particles Improve Their Ice Nucleation Ability? J. Phys. Chem. A, 118, 7330−7337, 2014a.

Lupi, L., Hudait, A., and Molinero, V.: Heterogeneous Nucleation of Ice on Carbon Surfaces. J. Am. Chem. Soc.,136, 3156−3164, 2014b.

Ma, X., Zangmeister, C. D., Gigault, J., Mulholland, G. W. and Zachariah, M. R.: Soot aggregate restructuring during

30   water processing, J. Aerosol Sci., 66, 209–219, doi:10.1016/j.jaerosci.2013.08.001, 2013.

Marcolli, C.: Deposition nucleation viewed as homogeneous or immersion freezing in pores and cavities, Atmos. Chem. Phys., 14(4), 2071–2104, doi:10.5194/acp-14-2071-2014, 2014.

Marcolli, C.: Pre-activation of aerosol particles by ice preserved in pores, Atmos. Chem. Phys., 17(3), 1595–1622, doi:10.5194/acp-17-1595-2017, 2017.

35   McCluskey, C. S., DeMott, P. J., Prenni, A. J., Levin, E. J. T., McMeeking, G. R., Sullivan, A. P., Hill, T. C. J., Nakao, S., Carrico, C. M. and Kreidenweis, S. M.: Characteristics of atmospheric ice nucleating particles associated with

biomass burning in the US: Prescribed burns and wildfires, J. Geophys. Res., 119(17), 10,458-10,470, doi:10.1002/2014JD021980, 2014.

Möhler, O., C. Linke, H. Saathoff, M. Schnaiter, R. Wagner, A. Mangold, M. Krämer, and U. Schurath: Ice nucleation on flame soot aerosol of different organic carbon content, Meteorol. Z., 14(4), 477–484, doi:10.1127/ 0941-2948/2005/0055, 2005.

Morishige, K.: Influence of Pore Wall Hydrophobicity on Freezing and Melting of Confined Water, J. Phys. Chem. C, acs.jpcc.8b00538, doi:10.1021/acs.jpcc.8b00538, 2018.

Murphy, D. M., D. J. Cziczo, K. D. Froyd, P. K. Hudson, B. M. Matthew, A. M. Middlebrook, R. E. Peltier, A. Sullivan, D. S. Thomson, and R. J. Weber: Single-particle mass spectrometry of tropospheric aerosol particles, J. Geophys. Res., 111, D23S32, doi:10.1029/2006JD007340, 2006.

Murr, L. E. and Soto, K. F.: A TEM study of soot, car- bon nanotubes, and related fullerene nanopolyhedra in common fuel-gas combustion sources, Mater. Charact., 55, 50–65, doi:10.1016/j.matchar.2005.02.008, 2005.

Petzold, A., Ström, J., Ohlsson, S. and Schröder, F. P.: Elemental composition and morphology of ice-crystal residual particles in cirrus clouds and contrails, Atmos. Res., 49(1), 21–34, doi:10.1016/S0169-8095(97)00083-5, 1998.

Phillips, V. T. J., Demott, P. J., Andronache, C., Pratt, K. A., Prather, K. A., Subramanian, R. and Twohy, C.: Improvements to an Empirical Parameterization of Heterogeneous Ice Nucleation and its Comparison with Observations. J. Atmos. Sci., 70:378–409, 2013.

Pósfai, M., J. R. Anderson, P. R. Buseck, and H. Sievering: Soot and sulfate aerosol particles in the remote marine troposphere, J. Geophys. Res., 104(D17), 21685–21693, doi: 10.1029/1999JD900208, 1999.

Pratt, K. A., DeMott, P. J., French, J. R., Wang, Z., Westphal, D. L., Heymsfield, A. J., Twohy, C. H., Prenni, A. J. and Prather, K. A.: In situ detection of biological particles in cloud ice-crystals, Nat. Geosci., 2, 398 [online] Available from: http://dx.doi.org/10.1038/ngeo521, 2009.

Roesch, M., Roesch, C. and Cziczo, D. J.: Dry particle generation with a 3-D printed fluidized bed generator, Atmos. Meas. Tech., 10(6), 1999–2007, doi:10.5194/amt-10-1999-2017, 2017.

Sakamoto, K. M., Laing, J. R., Stevens, R. G., Jaffe, D. A. and Pierce, J. R.: The evolution of biomass-burning aerosol size distributions due to coagulation: Dependence on fire and meteorological details and parameterization, Atmos. Chem. Phys., 16(12), 7709–7724, doi:10.5194/acp-16-7709-2016, 2016.

Seinfeld, J. H., and S. N. Pandis: Atmospheric Chemistry and Physics, Wiley-Interscience, Hoboken, N. J., 1998.

Ullrich, R., Hoose, C., Möhler, O., Niemand, M., Wagner, R., Höhler, K., Hiranuma, N., Saathoff, H. and Leisner, T.: A New Ice Nucleation Active Site Parameterization for Desert Dust and Soot, J. Atmos. Sci., 74(3), 699–717, doi:10.1175/JAS-D-16-0074.1, 2017.

Vali, G.: Interpretation of freezing nucleation experiments: singular and stochastic; sites and surfaces, Atmos. Chem. Phys., 14, 5271-5294, https://doi.org/10.5194/acp-14-5271-2014, 2014.

Vali, G., DeMott, P. J., Möhler, O., and Whale, T. F.: Technical Note: A proposal for ice nucleation terminology, Atmos. Chem. Phys., 15, 10263-10270, https://doi.org/10.5194/acp-15-10263-2015, 2015.

Vlahou, I. and Worster, M. G.: Ice growth in a spherical cavity of a porous medium, J. Glaciol., 56(196), 271–277, doi:10.3189/002214310791968494, 2010.

Vu, T. V, Delgado-Saborit, J. M. and Harrison, R. M.: Review: Particle number size distributions from seven major sources and implications for source apportionment studies, Atmos. Environ., 122, 114–132, doi:https://doi.org/10.1016/j.atmosenv.2015.09.027, 2015.

Wagner, R., Kiselev, A., Möhler, O., Saathoff, H. and Steinke, I.: Pre-activation of ice-nucleating particles by the pore
5 condensation and freezing mechanism, Atmos. Chem. Phys., 16(4), 2025–2042, doi:10.5194/acp-16-2025-2016, 2016.

Wang, B. and Knopf, D.A.: Heterogeneous ice nucleation on particles composed of humic-like substances impacted by O3, J. Geophys. Res. Atmos., 116(D3), doi:10.1029/2010JD014964, 2011.

Whale, T. F., Rosillo-Lopez, M., Murray, B. J. and Salzmann, C. G.: Ice Nucleation Properties of Oxidized Carbon
10 Nanomaterials, J. Phys. Chem. Lett., 6(15), 3012–3016, doi:10.1021/acs.jpclett.5b01096, 2015.

Wildeman, S., Sterl, S., Sun, C. and Lohse, D.: Fast Dynamics of Water Droplets Freezing from the Outside in, Phys. Rev. Lett., 118(8), 1–5, doi:10.1103/PhysRevLett.118.084101, 2017.

Wolf, M.J., Coe, A., Dove, L.A., Zawadowicz, M.A., Dooley, K., Biller, S.J., Zhang, Y., Chisholm, S.W., Cziczo, D.J.: Investigating the Heterogeneous Ice Nucleation Potential of Sea Spray Aerosols Using Prochlorococcus as a
15 Model Source of Marine Organic Matter. Submitted to J. Env. Sci. Tech., submitted, 2018.

Zangmeister, C. D., Radney, J. G., Dockery, L. T., Young, J. T., Ma, X., You, R. and Zachariah, M. R.: Packing density of rigid aggregates is independent of scale, Proc. Natl. Acad. Sci., 111(25), 9037–9041, doi:10.1073/pnas.1403768111, 2014.

Zawadowicz, M. A., Abdelmonem, A., Mohr, C., Saathoff, H., Froyd, K. D., Murphy, D. M., Leisner, T. and Cziczo,
20 D. J.: Single-Particle Time-of-Flight Mass Spectrometry Utilizing a Femtosecond Desorption and Ionization Laser, Anal. Chem., 87(24), 12221–12229, doi:10.1021/acs.analchem.5b03158, 2015.

Zhou, C. and Penner, J. E.: Aircraft soot indirect effect on large-scale cirrus clouds: Is the indirect forcing by aircraft soot positive or negative? J. Geophys. Res. Atmos. 119(19): 11, 303-11, 320, doi: 10.1002/2014JD021914, 2014.

Zhu, W., Zhu, Y., Wang, L., Zhu, Q., Zhao, W., Zhu, C., Bai, J., Yang, J., Yuan, L.-F., Wu, H.-A. and Zeng, X. C.:
25 Water Confined in Nanocapillaries: Two-Dimensional Bilayer Square-like Ice and Associated Solid-Liquid-Solid Transition, J. Phys. Chem. C, acs.jpcc.8b00195, doi:10.1021/acs.jpcc.8b00195, 2018.

Zobrist, B., Marcolli, C., Koop, T., Luo, B. P., Murphy, D. M., Lohmann, U., Zardini, A. A., Krieger, U. K., Corti, T., Cziczo, D. J., Fueglistaler, S., Hudson, P. K., Thomson, D. S., and Peter, T.: Oxalic acid as a heterogeneous ice nucleus in the upper troposphere and its indirect aerosol effect, Atmos. Chem. Phys., 6, 3115-3129,
30 https://doi.org/10.5194/acp-6-3115-2006, 2006.

Atmospheric
Chemistry
and Physics
Discussions

Open Access

Table 1. Aerosol materials with selected properties. BET, OAN, and surface type information is provided by the manufacturer and pertain to bulk properties. The data in the last four columns were collected in our laboratory; pH was measured for the bulk suspensions; effective density (ρ_{eff}), O:C ratio, and OPC data were collected for dry dispersed BC particles.

Sample	[a]BET [m² g⁻¹] (manufacturer)	[b]OAN [ml/100 g] (manufacturer)	Surface type (manufacturer)	[c]pH	[d]ρ_{eff} [g cm⁻³]	[e]PALMS median O:C ratio (Fig. A1)	[f]OPC Log(S1), Log(P1)
Regal 330R	90	65	Non-oxidized	6.9	0.79	0.018	2.4, 3.3
Regal 400R	90	70	Oxidized	4.9	1.24	0.057	2.3, 3.2
Monarch 880	240	110	Non-oxidized	6.7	0.76	0.015	1.4, 2.9
Monarch 900	240	70	Non-oxidized	6.8	0.84	0.024	1.4, 2.9
Raven 2500 Ultra	270	67	----------	7.0	1.12	0.036	1.4, 2.8
Ethylene combustion soot	----------	------------	----------	6.4	0.59	0.037	2.0, 3.1

5   [a]BET (Brunauer–Emmett–Teller) method measures the surface adsorption area to mass ratio of the bulk powder.

[b]OAN (Oil Absorption Number) is proportional to the absorbed oil volume to mass ratio of the bulk powder.

[c]pH measured for bulk suspension of BC materials.

[d]ρ_{eff} is the effective density calculated from the ratio of the vacuum aerodynamic diameter (D_a) measured by the PALMS (Particle-Analysis-by-Laser-Mass-Spectrometry) instrument and the constant mobility diameter (D_m) of 800

10   nm, multiplied by the standard density of 1 g cm⁻³.

[e]Median O:C ratio measured by PALMS instrument for selected mobility diameter (D_m) of 800 nm.

[f]OPC Optical Particle Counter. Logarithmic values of parallel (S1) and perpendicular (P1) polarization, measured by the OPC for size selected 800 nm mobility samples, are shown in the last column.
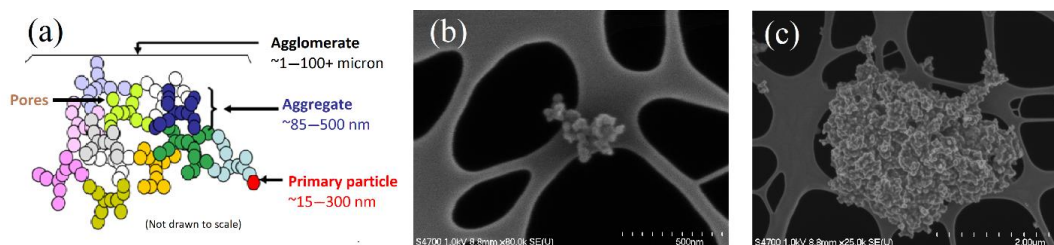
Figure 1. (a) Illustration of agglomerate, aggregate, and spherule definitions, reproduced with permission from Long et al. (2013). Electron microscope images of (b) Soot aggregate on a substrate, and (c) soot agglomerate on a substrate.
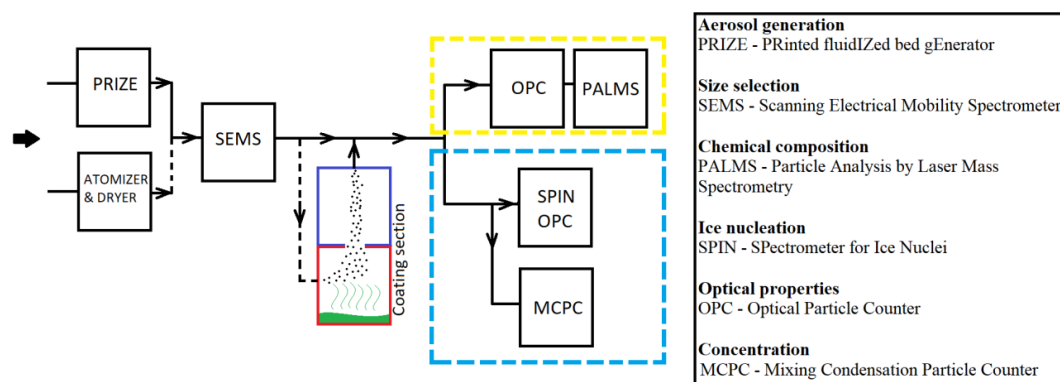
5   **Figure 2. Simplified diagram of the apparatus showing aerosol generation, coating, characterization (yellow dashed frame), and ice nucleation measurements (blue dashed frame). The red frame is the flask containing the organic acid, which was heated to a temperature slightly lower than the onset of homogeneous particle nucleation of organic compounds. The blue frame is a chilled condenser (-20 °C) which promotes condensation of organic acids on BC.**
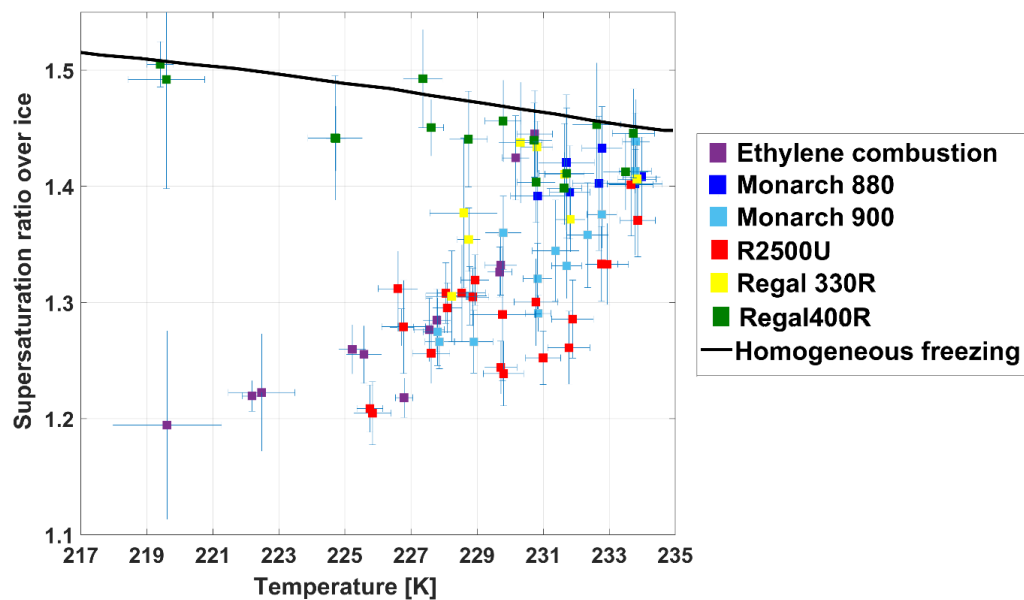
Figure 3. Ice onset by heterogeneous nucleation from 800 nm BC particles at supersaturated conditions w.r.t. ice in the temperature range 217 to 235 K by 1 % of the particles. Solid black line is the homogeneous freezing threshold (Koop et al., 2000).

Atmospheric
Chemistry
and Physics
Discussions
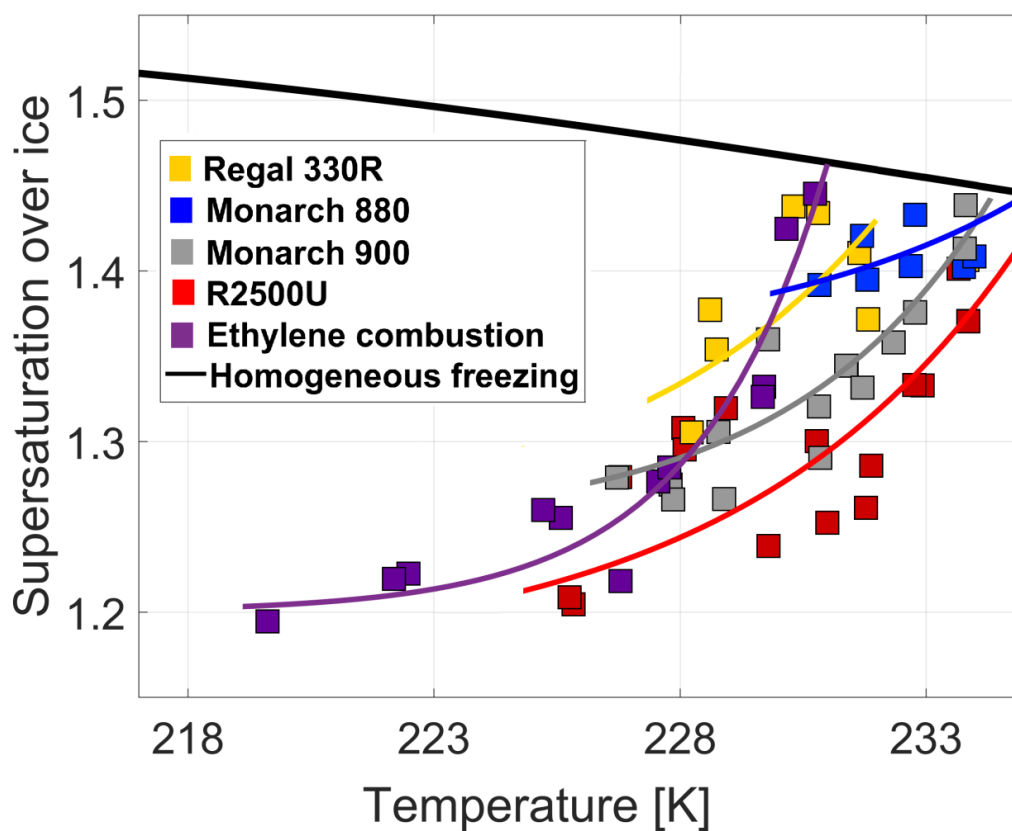
Figure 4. Morphological effect on ice activity of 800 nm BC particles (Factor 1 in the Introduction). The solid color-coded lines fitted to the data sets are only guides to the eye. The black solid line is the homogeneous freezing threshold.
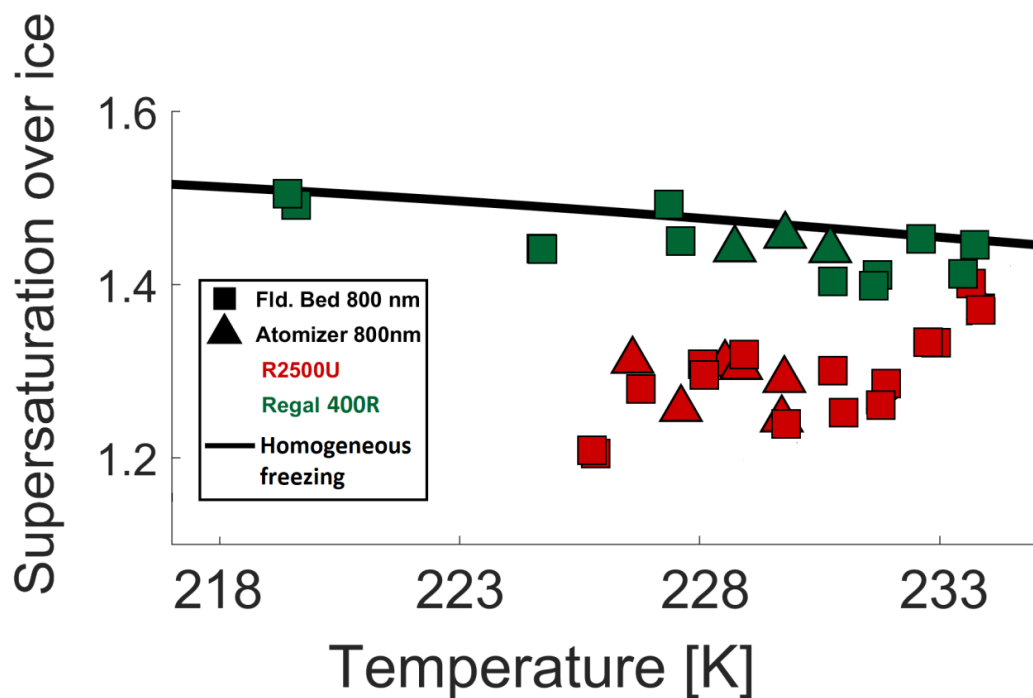
Figure 5. Aerosol generation technique effect on IN activity. The black solid line is the homogeneous freezing threshold.
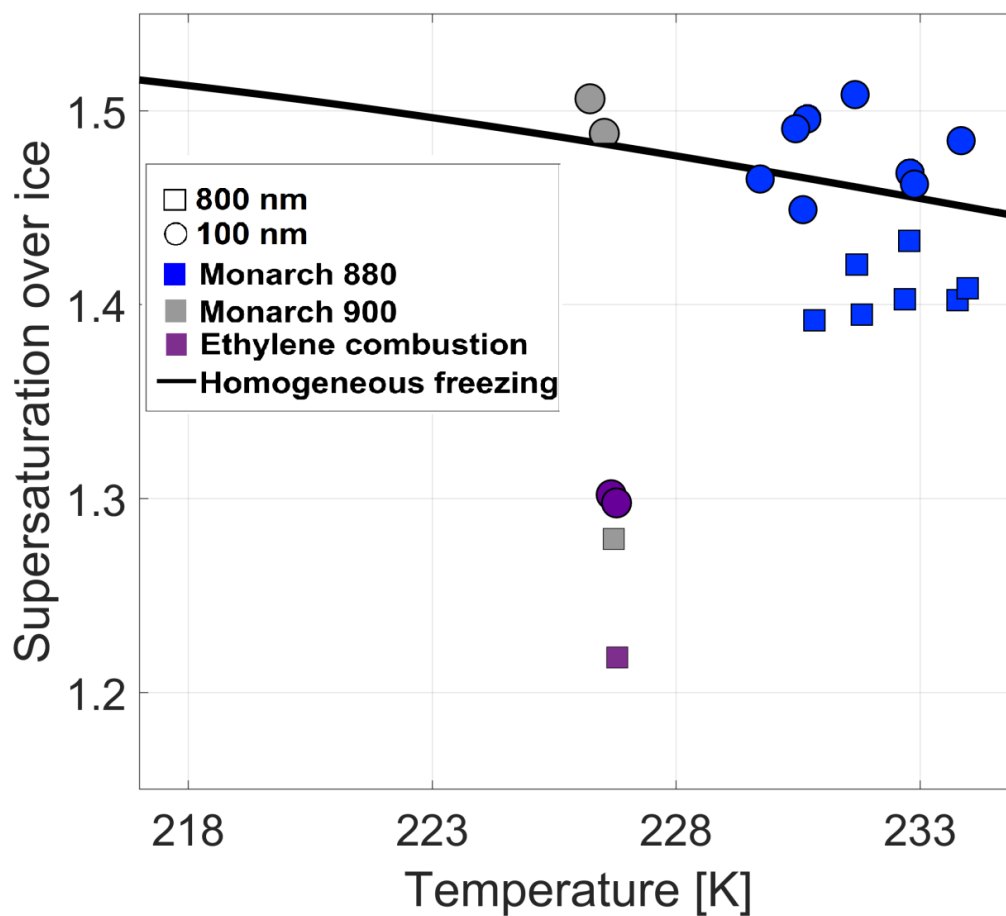
Figure 6. Effect of particle size on ice onset (Factor 2 in the Introduction). Squares represent data obtained with 800 nm particles, circles represent 100 nm particle data. The black solid line is the homogeneous freezing threshold.

Atmospheric
Chemistry
and Physics
Discussions
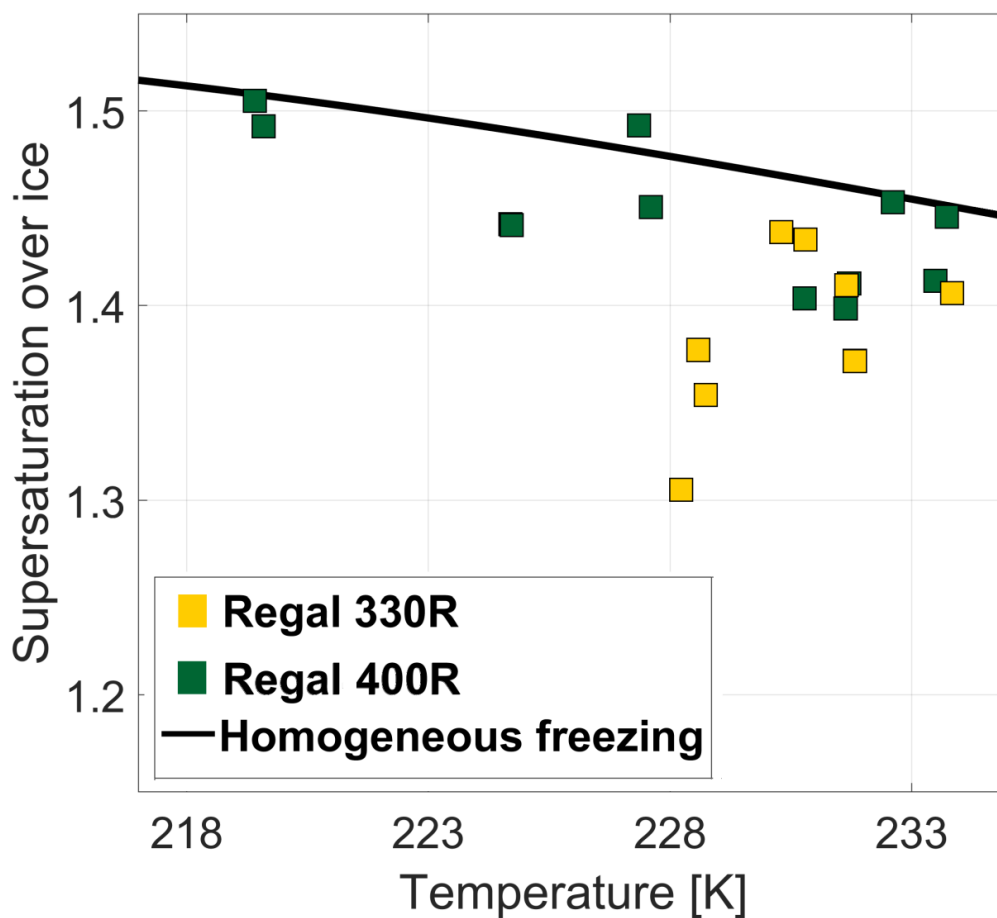
Figure 7. Influence of surface oxidation on IN activity (Factor 3 in the Introduction). Comparison of 2 BC compounds with identical BET and comparable OAN values (Table 1), mainly differing in the degree of surface oxidation (Fig. A1). The black solid line is the homogeneous freezing threshold.

Atmospheric
Chemistry
and Physics
Discussions

Open Access
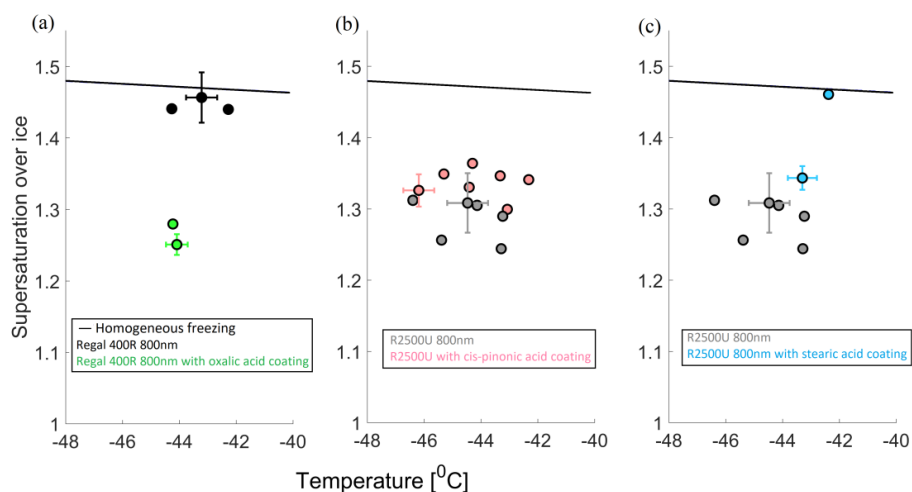
Figure 8. Modification of ice nucleation onset on BC particles by organic coating. (a) oxalic acid on Regal 400R. (b) cis-pinonic acid on R2500U. (c) stearic acid on R2500U.
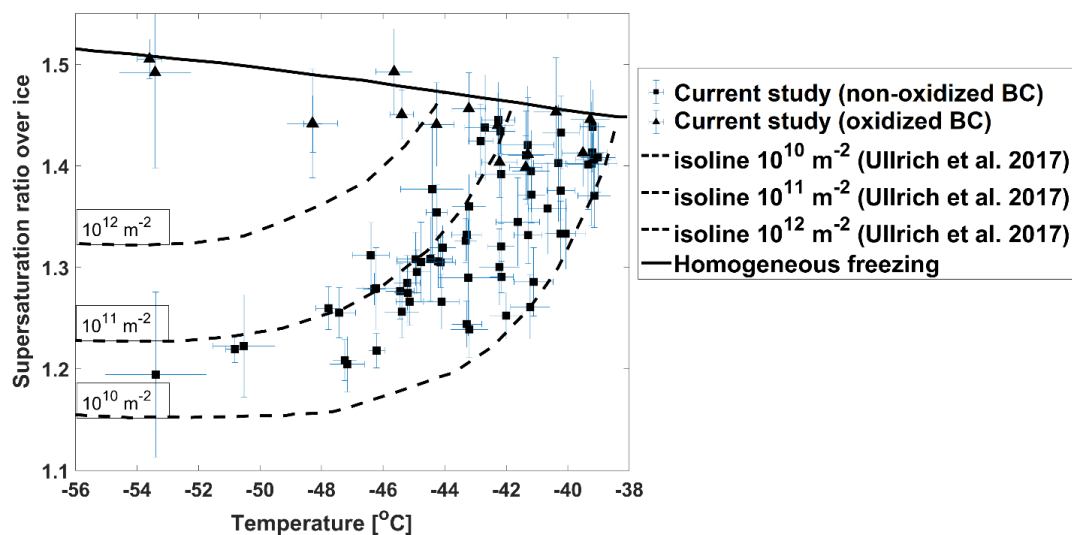
5   **Figure 9. Ice nucleation on 800 nm BC particles at supersaturated conditions w.r.t. ice in the temperature range 217 to 235 K by 1 % of the particles. Experimental data of BC samples plotted together with active site density isolines reproduced from empirical parametrization of soot IN activity by Ullrich et al. (2017). The black solid line is the homogeneous freezing threshold.**
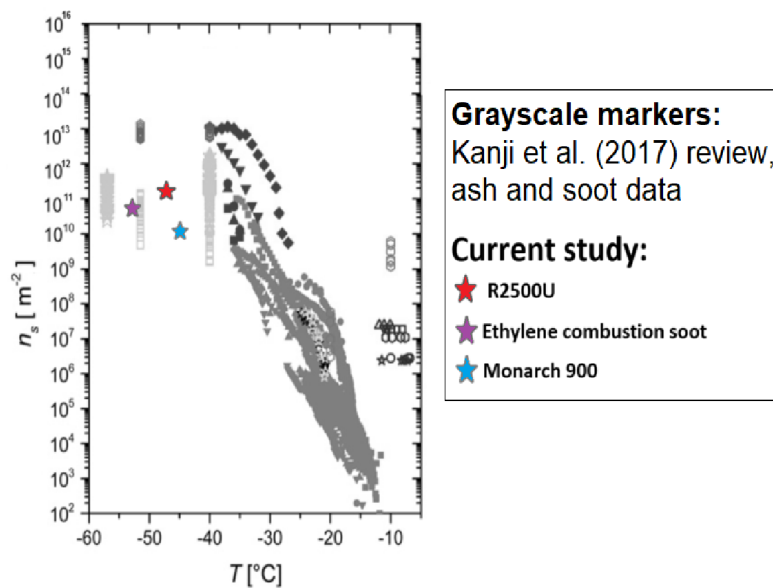
Figure 10. Active site density (n_s) as a function of temperature of three selected results of the most active IN in this study that complement the data on a figure reproduced from Kanji et al. (2017) (grayscale) and references therein. Red star is R2500U, purple star is ethylene combustion soot, and turquoise star is Monarch 900.

Atmospheric
Chemistry
and Physics
Discussions

Open Access

EGU
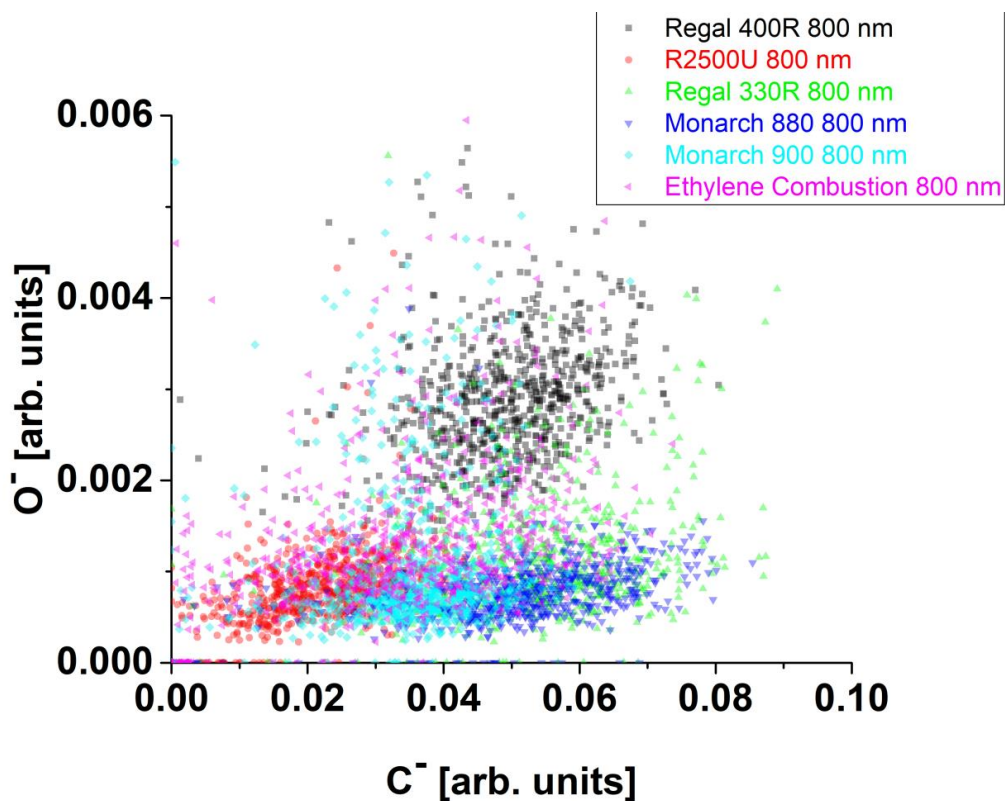
Figure A1. Negative oxygen ion peak area plotted against carbon negative ion peak area derived from ~1000 single particle spectra of each BC sample (color-coded). Regal 400R appears to have the highest O⁻ content.
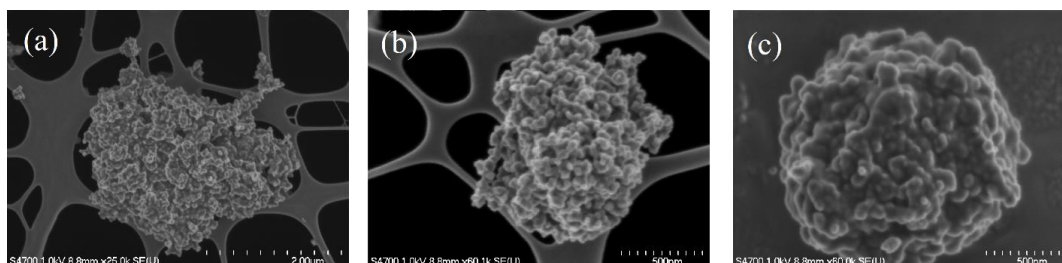
5   **Figure A2. Selected electron microscope images of dry dispersed agglomerates of (a) Ethylene combustion product, (b) Regal 400R, (c) Raven 2500 Ultra. Most often occurring shape is compacted spheroidal.**